Limnol. Oceanogr., 49(1), 2004, 86–94

Anaerobic N_2 production in Arctic sea ice

Søren Rysgaard[1]
National Environmental Research Institute, Department of Marine Ecology, Vejlsøvej 25, DK-8600 Silkeborg, Denmark

Ronnie Nøhr Glud
Marine Biological Laboratory, University of Copenhagen, Strandpromenaden 5, DK-3000 Helsingør, Denmark

Abstract

We quantified anaerobic N_2 production through bacterial denitrification and anaerobic NH_4^+ oxidation (anammox) in first-year ice from Young Sound (74°N) and in an ice floe off Northeast Greenland (79°N). Bacterial denitrification activity (100–300 nmol N L^{-1} sea ice d^{-1}) occurred in the lower 0.5 m of the sea ice, which had high concentrations of NO_3^-, NH_4^+, and dissolved organic carbon (DOC). Despite sea-ice algal production in the lower sea-ice layers, heterotrophic activity resulted in a net O_2 consumption of 13 μmol O_2 L^{-1} sea ice d^{-1} in the lower 0.5-m ice layers. Together with melting of deoxygenated ice crystals, this led to anoxic conditions in the brine system favoring conditions for anaerobic NO_3^- reduction. Numbers of anaerobic NO_3^--reducing bacteria in the same ice layers were high (1.1×10^5 cells ml^{-1} sea ice, corresponding to 1.2×10^6 cells ml^{-1} brine). Area-integrated denitrification rates were 10–45 μmol N m^{-2} sea ice d^{-1}, which corresponds to 7–50% of the sediment activity in the area. Although the proportion of anammox to total N_2 production was up to 19% in layers of the ice floe from the Greenland Sea, the integrated rate only accounted for 0–5% of total NO_3^- reduction at the investigated localities.

With a global average extent of $19–29 \times 10^6$ km^2 (Gloersen et al. 1992), sea ice provides a vast low-temperature habitat for many species of bacteria, fungi, algae, protozoa, and metazoa. Accumulation of temporary intermediate compounds of the nitrogen cycle, such as NO_3^-, NO_2^-, and NH_4^+, is frequently observed in sea ice (Thomas et al. 1995; Kaartokallio 2001). Furthermore, high dissolved organic carbon concentrations in conjunction with high NH_4^+ levels in Arctic sea ice indicate that a significant proportion of the dissolved organic matter is a result of degradation of ice algae and/or detritus originally incorporated during ice formation (Thomas et al. 1995). Recently, exopolymeric substances (EPS) found in very high concentrations in the brine system appear to play an important buffering and cryoprotectant role for microorganisms, especially diatoms (Krembs et al. 2002). These substances may represent a previously unrecognized source of organic matter for heterotrophic activity.

High concentrations of NO_3^- and organic carbon in local anoxic microsites create optimal conditions for bacterial nitrogen reduction. Denitrification is known to occur in microsites surrounded by fully aerobic conditions, e.g., water-filled soil pores (Tiedje 1988). Aerobic heterotrophic respiration with the available organic carbon is the major mechanism removing oxygen from these microsites (Tiedje 1988). Recently, it has been suggested that O_2 depletion may occur in association with ice thaw due to liberation of O_2-depleted meltwater and that it may create favorable conditions for anaerobic bacteria and processes within the sea-ice matrix (Glud et al. 2002). Furthermore, genetic analysis of sea-ice bacterial communities in the Baltic Sea have revealed the presence of anoxygenic phototrophic purple sulfur bacteria, indicating the existence of oxygen-deficient and anoxic zones or niches in sea ice (Petri and Imhoff 2001).

Bacterial strains of denitrifying species have been isolated from Antarctic sea ice (Staley and Gosink 1999). However, whereas numerous investigations of bacterial denitrification have been reported from soil and sediment systems (Højberg et al. 1994; Devol et al. 1997; Rysgaard et al. 1998), we are only aware of one study from sea-ice systems. Cultures isolated from sea ice in the Baltic Sea exhibited the highest denitrification activity, i.e., the highest N_2O production, when extracted from interior layers of 2–3-month-old sea ice (Kaartokallio 2001). The elevation in denitrification activity was associated with accumulation of NO_2^-, and heterotrophic organisms composed 7–20% of the organism assemblage.

Previously, denitrification was recognized as the only important process removing nitrogen from natural environments. However, it has recently been discovered that ammonium is oxidized anaerobically in sediments in the presence of NO_2^- and that this alternative pathway may significantly contribute to natural sediment N_2 production (Thamdrup and Dalsgaard 2002; Dalsgaard and Thamdrup 2002). Although limited knowledge exists on this new pathway from natural systems, it has been shown in a temperate site that anaerobic NH_4^+ oxidation has a lower temperature optimum than denitrification and potentially could be favored in colder systems such as Arctic sediments and sea ice (Dalsgaard and Thamdrup 2002).

Here we provide the first quantification of denitrification

[1] Corresponding author (sr@dmu.dk).

Acknowledgments

The crew on the Danish military vessel *Vædderen* is thanked for their enthusiasm and help with sampling. The military sledge patrol Sirius is thanked for their hospitality and help in general. We thank Tanja Quottrup, Kitte Gerlich, Marlene Skjærbæk, Egon Frandson, and Anna Haxen for excellent assistance in the laboratory back in Denmark. Kai Finster is acknowledged for help with the enumeration of bacteria. Finally, we thank two anonymous reviewers for constructive comments that improved the manuscript.

This study was financially supported by the Danish Research Councils, and by DANCEA, the Danish Cooperation for Environment in the Arctic, Danish Ministry of Environment.

and anaerobic ammonium oxidation in natural sea-ice samples. Activities are discussed in relation to oxygen conditions, ice algal production, dissolved organic carbon (DOC), and nutrient conditions during the onset of ice melt in a coastal first-year sea-ice location, Young Sound (74°N), supplemented with measurements from an ice floe off Northeast Greenland (79°N).

Materials and methods

Study sites—The investigation covers measurements on sea ice from Young Sound, a northeastern Greenland fjord (74°18.59′N, 20°15.04′W—water depth 36 m). Sampling of 1.5-m-thick first-year ice was performed from 28 May to 12 June 2002. In this locality, sea ice usually begins to form in September and increases in thickness to ~1.5 m in the course of April–May. The ice typically breaks in mid–late July. Further details on sea ice and associated microbial activity in Young Sound are available elsewhere (Rysgaard et al. 2001; Glud et al. 2002). Supplementary investigations of bacterial N_2 production in a 2.2-m-thick ice floe in the Greenland Sea (79°21.16′N, 11°08.50′W—water depth 265 m) were made mid-September 2002 from the Danish military vessel *Vædderen.*

Sea ice—Sea ice was drilled with a MARK II coring system (Kovacs Enterprises). At each sampling session, vertical temperature profiles were measured with a thermometer (Testo thermometer) in the center of the cores through 3-mm holes drilled immediately after coring. Sea ice was then cut into 5–10-cm sections and kept cold (0°C) and brought to the field laboratory within 1–2 h for further processing. In the laboratory, sea ice was melted within 2 h, GF/F filtered and frozen (−18°C) until nutrient analysis. Filters were extracted for 24 h in 96% ethanol and analyzed fluorometrically for chlorophyll *a* (10-AU Turner design fluorometer). Salinity of the melted sections was determined with a sonde (Knick konduktometer) calibrated to a PORTASAL salinometer. Brine and gas volumes in sea ice were calculated according to Cox and Weeks (1983) for temperatures below −2°C, and according to Leppäranta and Manninen (1988) for temperatures within the range 0°C to −2°C. Concentrations of $NO_3^- + NO_2^-$, and NH_4^+ were analyzed by standard techniques (Grasshoff et al. 1983). DOC samples were filtered (combusted GF/Fs) and analyzed with a Shimadzu DOC-5000 Analyzer. DOC calibrations were made with 45-μl injections of potassium hydrogen phthalate ($C_8H_5KO_4$) in ultraviolet-oxidized Q-water. All carbon data were corrected for instrument blank of 12 μmol L^{-1}, and each measurement represents the mean of 3–7 injections.

On each occasion, a parallel set of cores was sampled and cut into sections as described above. From each section, the central part (50–80 g) was cut free by removing an equal thickness of ice from all sides of the section and immediately placing it in a 200-ml gas-tight glass syringe fitted with a 50-cm gas-tight Tygon tube. Artificial seawater (50–80 ml; Grasshoff et al. 1983) with a known O_2 concentration, as determined by Winkler titration, was then added, and the syringe immediately closed with a piston and a clamp. Incubations of artificial water showed no bacterial O_2 consumption (data not shown). The syringes were submersed in cold melted snow and kept cold (0°C) and brought to the field laboratory within 1–2 h. In the laboratory, the ice in the syringes was melted within 2 h and the gas volumes measured (at 2°C) from the length and diameter of the gas after moving it into the transparent Tygon tube (inner diameter, 3 mm). During the melting procedure, O_2 in the bubbles was equilibrated with the melted sea ice by vigorously shaking the syringe. The gas bubble was then transferred to a gas-tight vial (Exetainer®, Labco) containing helium-flushed water (free of O_2) and $ZnCl_2$ (200 μl of a 50% w/v solution) until later analysis. The O_2 concentration in the remaining melted sea ice/water sample was determined by Winkler titration, and the O_2 concentration in the gas was determined on a gas chromatograph coupled to a triple-collector isotopic ratio mass spectrometer (RoboPrep-G+ in line with Tracermass). The total amount of O_2 in the sea ice was calculated from the amount of O_2 in the melted sample and gas minus the amount initially added with the artificial seawater.

In parallel to the two sets of cores described above, a third set of cores was sampled and also cut into 5–10-cm sections. These were likewise kept cold and brought to the field laboratory within 1–2 h. In the laboratory, the sections were melted and each melted section was flushed with helium to remove all O_2 in the sample, mainly originating from the entrapped gas bubbles and the sampling treatment. Three treatments were performed: (a) addition of 50 μmol L^{-1} $^{15}NO_3^-$ (99.6 atom %), (b) addition of 50 μmol L^{-1} $^{15}NH_4^+$ (99.6 atom %), and (c) addition of 50 μmol L^{-1} $^{15}NH_4^+$ (99.6 atom %) and 50 μmol L^{-1} $^{14}NO_3^-$ (0.367 atom %). The anoxic melted sea ice containing the three different isotopic treatments was then transferred to gas-tight vials (Exetainer®) and incubated at different time intervals at 0°C in the dark. At four different time intervals (after 0.5–7 d of incubation), incubation was stopped by introducing a 4-ml helium headspace and adding 200 μl of a $ZnCl_2$ solution (50% w/v) to preserve samples until later analysis. The 4-ml sample withdrawn while introducing the 4-ml helium headspace was frozen (−18°C) until later isotope analysis. The abundance and concentration of $^{14}N^{15}N$ and $^{15}N^{15}N$ were analyzed on a gas chromatograph coupled to a triple-collector isotopic ratio mass spectrometer (RoboPrep-G+ in line with Tracermass, PDZ Europa) as described by Risgaard-Petersen and Rysgaard (1995). The isotopic distributions in the NO_3^- and NH_4^+ pools were likewise analyzed by mass spectrometry after reduction to N_2 according to the procedures of Risgaard-Petersen and Rysgaard (1995). Production of N_2 through denitrification and N_2 production by anaerobic NH_4^+ oxidation (anammox) was calculated according to Nielsen (1992) and Thamdrup and Dalsgaard (2002), respectively.

In addition to the sampling described above, seven cores were recovered 28 May in Young Sound, and the bottom 30 cm of each sea-ice core was enclosed in a transparent gas-tight laminated NEN/PE plastic bag (Hansen et al. 2000). A small amount of artificial sea water (Grasshoff et al. 1983) with a known O_2 concentration (Winkler measurement) was added to each bag in order to remove bubbles trapped between the ice core and the plastic wall. The bags were then closed and returned to their respective holes in the sea ice

and incubated in situ. At different time intervals (0–12 d), a core was brought back to the field laboratory and melted, and the total content of entrapped O_2 in gas bubbles and in melted sea ice was determined as described above.

In combination with the O_2 measurements in the gas-tight bags, primary production measurements were made on subsamples of the melted sea ice using ^{14}C. In short, melted sea ice was added to two light bottles and 1 dark (3×120 ml) together with 4 μCi $H^{14}CO_3$ and incubated around noon in the opening in the sea ice close to the sea-ice/water column interface for 2 h. After incubation, the bottles were kept in the dark until filtration, which was performed within 2 h. The entire content of each bottle was filtered onto 25-mm GF/F filters. The filters were transferred to scintillation vials together with 200 μl of 1 N HCl and then frozen until counting. Excess inorganic ^{14}C was removed by directing a flow of air into the vials before addition of scintillation fluid. Samples were counted on a liquid scintillation analyzer (Packard 1990TR). The concentration of dissolved inorganic carbon (DIC) was measured on the melted sea-ice samples using a CO_2 analyzer (Coulometer CM5012, UIC Inc.). Carbon fixation was derived after subtracting the dark fixation values.

Denitrifying bacteria—Nitrate-respiring bacteria from ice samples were enumerated in dilution series. Each series contained 3×6 tubes. The enumerations were carried out using 16-ml Hungate tubes supplemented with 9 ml of oxygen-free carbonate-buffered saltwater medium (Widdel and Bak 1992). Tryptic Soy Broth (TSB) served as energy and carbon source and nitrate or nitrite as electron acceptor. Three enumerations were carried out with the following substrate combinations: (I) 2 g TSB L^{-1} and 5 mmol L^{-1} KNO_3. (II) 10 g TSB L^{-1} and 10 mmol L^{-1} KNO_3. (III) 2 g TSB L^{-1} and 5 mmol L^{-1} KNO_2. The inoculum was obtained from a 30-cm bottom section of an ice core sampled on 3 June. The ice core was melted under avoidance of oxygenation by bubbling with helium. One ml of the meltwater was injected into the first tube with a syringe through the rubber septum that sealed the tube. The first tube was mixed and 1 ml was withdrawn with a new syringe and injected into the next tube. This procedure was followed to inoculate all enumeration tubes. In the laboratory, the tubes were incubated in the dark at 5°C and scored 8 weeks after inoculation. All tubes were checked for growth by microscopy and by determining the consumption of nitrate and nitrite and gas production. To check that NO_3^- was reduced all the way to N_2 in the enumeration tubes, an inoculum from media II and III of the intermediate dilution series was dark incubated in oxygen-free carbonate-buffered saltwater medium containing 5 g TSB L^{-1} and 50 μmol L^{-1} $^{15}NO_3^-$ (99.6 atom %). After an incubation period of 24 h, these were analyzed for ^{15}N-N_2 production on a gas chromatograph coupled to a triple-collector isotopic ratio mass spectrometer (RoboPrep-G+ in line with Tracermass, PDZ Europa).

Results

On arrival to the Young Sound locality at the end of May, a ~40-cm snow layer covered the fjord. The snow cover decreased during the study period from 28 May–12 June ($r^2 = 0.94$, $P \ll 0.001$), representing a meltwater production of 6 ± 0.7 mm d^{-1} (water equivalent, density assumed to be 300 kg m^{-3}) (Fig. 1). A clear, solid, freshwater ice layer ~5 cm thick was found immediately below the snow layer and persisted until 9 June, when it broke. Below the freshwater ice layer, a 6–15 cm, soft, partly melted ice layer of low salinity was present (Fig. 1). Sea-ice thickness did not change in the course of the study period ($r^2 = 0.002$, $P > 0.9$) but remained at a mean thickness of 146 ± 2.5 cm. Small meltwater ponds began to emerge on the sea-ice surface toward the end of the study period.

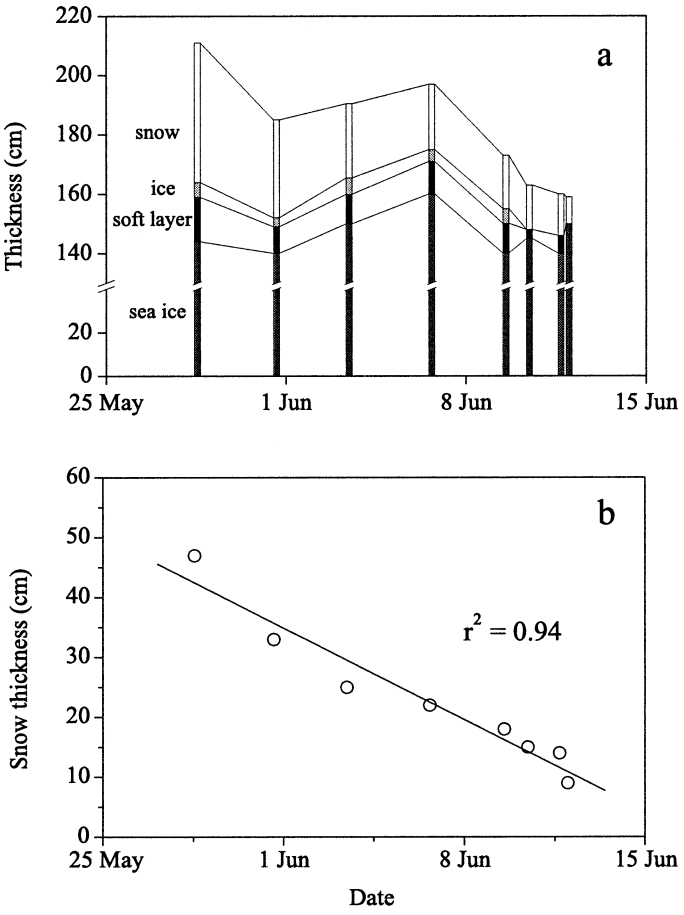

Fig. 1. (a) Snow and sea-ice conditions in the first-year ice location in Young Sound 2002. (b) Snow cover decreased linearly ($r^2 = 0.94$, $P \ll 0.001$) during the investigation period.

Ice temperatures in Young Sound ranged from −2.5°C to −0.3°C, with lowest temperatures observed in the center of the sea-ice matrix (Fig. 2a). Bulk salinities in Young Sound ranged from 0 to 7 (Fig. 2b) and the relative brine volume from 0.02 to 0.45, with high values in the bottom part of the ice during the final sampling dates (Fig. 2c). In the bottom 50 cm of the sea ice, temperature increased ($r^2 = 0.88$, $P < 0.001$) together with brine volume ($r^2 = 0.63$, $P = 0.02$) during the study period due to gradual melting of the sea ice (Fig. 3a). In the same ice layer and during the same period, a decrease in bulk salinity ($r^2 = 0.80$, $P = 0.002$) and brine salinity ($r^2 = 0.86$, $P < 0.001$) was observed (Fig.

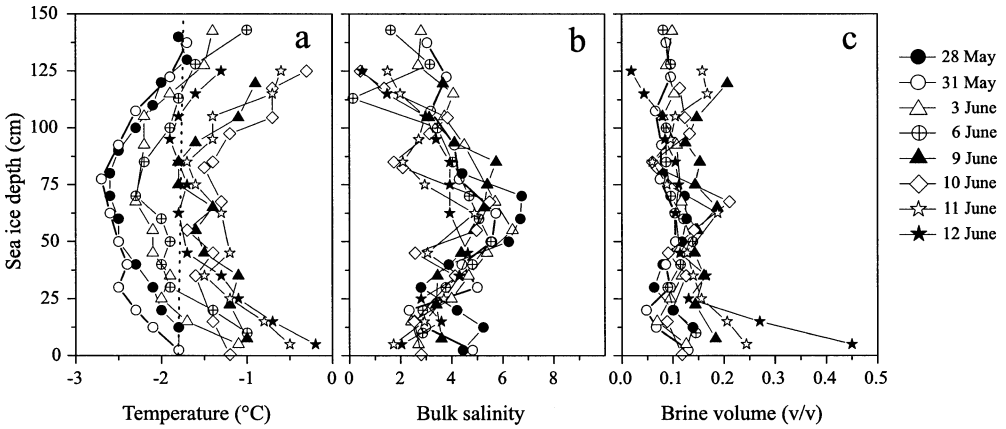

Fig. 2. (a) Temperature, (b) salinity, and (c) brine volume in ~1.5-m-thick sea ice from Young Sound. Sea-ice–water interface at 0 cm. Different symbols represent sea ice cores sampled on different dates during May–June 2002.

3b). On 15 September, temperature in the investigated ice floe in the Greenland Sea ranged from −1.3°C to −0.9°C and bulk salinities from 2 to 5 while the relative brine volume was 0.1–0.2 in the upper and bottom parts of the sea ice, respectively (data not shown).

Sea-ice Chl *a* values ranged from 0 to 15 μg L^{-1}, with the highest concentrations in the bottom 25 cm of the ice (Fig. 4a). However, Chl *a* was also present in the interior parts of the sea ice although in lower concentrations (up to 2–3 μg L^{-1}). Bulk concentrations of DOC in the sea ice ranged from 50 to 400 μmol L^{-1} (Fig. 4b). Nitrate was present throughout the sea-ice matrix of Young Sound, with a tendency toward increased concentrations in the bottom 25 cm. Bulk concentrations ranged from 0.2 μmol L^{-1} to 8 μmol L^{-1}, but no clear trend in development was observed during the study period, except for high values in bottom layers on the initial sampling date (Fig. 4c). Ammonium was also present throughout the ice matrix, ranging from 0.5 μmol L^{-1} to 7 μmol L^{-1} (Fig. 4d).

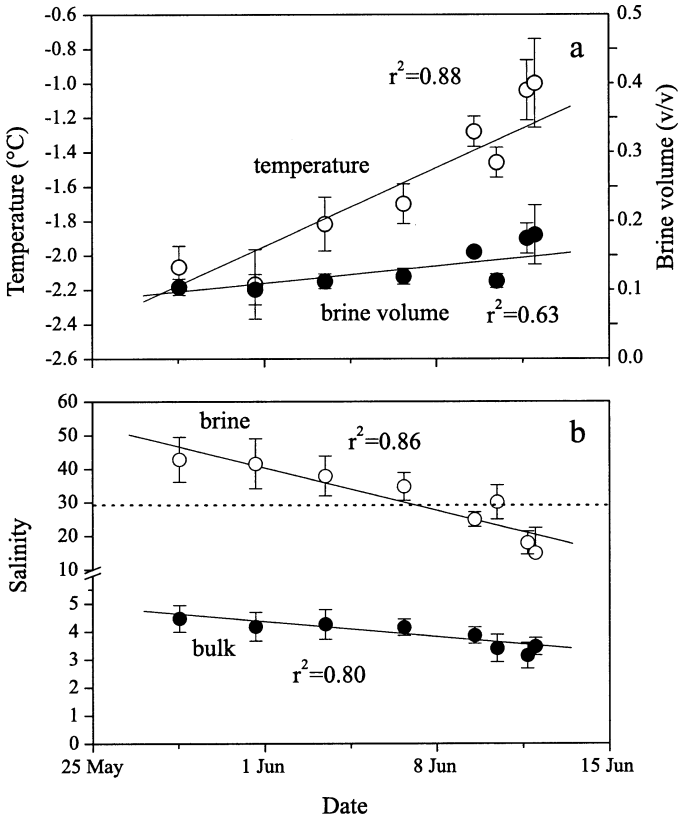

Fig. 3. (a) Temperature and brine volume conditions and (b) bulk and brine salinity in the bottom 50 cm of the sea ice from Young Sound during the investigation period.

Bubble (gas) volume showed a clear trend with small volumes (0–20 cm^3 L^{-1} sea ice) in the lower 50–60 cm of the sea ice and increasing volumes in the upper sea-ice layers (70–130 cm^3 L^{-1} sea ice; Fig. 5a). Measured bubble volumes were lower than expected (calculated according to Cox and Weeks [1983]) in the lower parts of the sea ice, presumably due to upward bubble transport. The total oxygen concentration in sea ice (O_2 in melted sea ice + O_2 in bubbles) followed the same trend as the bubble volume, with low (0–200 μmol L^{-1}) concentrations in the lower 50–60 cm of the ice matrix and higher (200–600 μmol L^{-1}) concentrations in the upper layers (Fig. 5b). The O_2 concentration in the sea ice was positively correlated with the gas volume within the sea ice in the beginning of the study period (28 May–3 June; $P < 0.001$, $r^2 = 0.78$–0.88), indicating that most O_2 present in the sea ice at this time was trapped in bubbles (Fig. 6). The strength of this correlation decreased from 6 June to 12 June ($P > 0.1$, $r^2 = 0.29$–0.03) (data not shown).

Primary production in the bottom 30 cm of the sea ice varied from 0.5 μmol C L^{-1} sea ice day^{-1} to 2 μmol C L^{-1} sea ice day^{-1}, with a calculated average of 1.7 ± 0.4 (standard error [SE], $n = 5$) μmol C L^{-1} sea ice day^{-1} (Fig. 7). Despite primary production in the sea ice, oxygen concentrations in the sea ice within the transparent gas-tight bags decreased during the incubation period (Fig. 7). After approximately 1 week of incubation, all O_2 was consumed. Linear regression of the data gives a net O_2 uptake of 13.0 μmol L^{-1} sea ice day^{-1} ($r^2 = 0.95$, standard deviation [SD] 10.7, $P = 0.013$). On average, the gross O_2 consumption

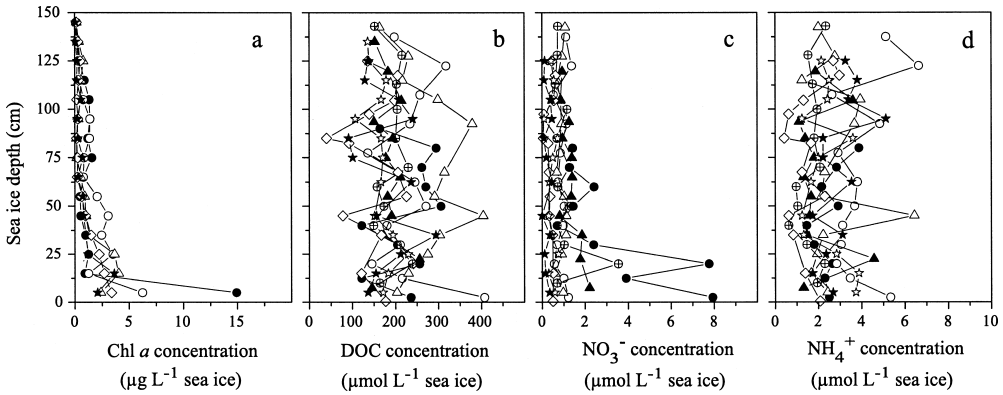

Fig. 4. (a) Concentrations of Chlorophyll *a*, (b) dissolved organic carbon (DOC), (c) nitrate, and (d) ammonium in Young Sound sea ice. Symbols as in Fig. 2.

amounts to 13.0 + 1.7 = 14.7 μmol L^{-1} sea ice day^{-1} during the May–June study period assuming a photosynthetic quotient of one.

Bacterial denitrification activity was observed in both Young Sound first-year ice and in Greenland Sea ice floes (Fig. 8). Except for one observation at 75 cm in Young Sound, highest activities were found in the lower 25 cm of the sea ice in both sea-ice types. Rates ranged from 0 nmol N L^{-1} d^{-1} to 100 nmol N L^{-1} d^{-1} in Young Sound and from 0 nmol N L^{-1} d^{-1} to 350 nmol N L^{-1} d^{-1} in the Greenland Sea location. Decreasing trends in activities during May–June were observed at the Young Sound locality (Fig. 8a). The proportion of anammox to total anaerobic N_2 production in Young Sound was below the detection limit but ranged from 0% to 19% in the bottom 60 cm of the Greenland Sea ice floe (Fig. 8b).

Bacterial growth was observed in all anaerobic Hungate tubes, giving a minimum average number of bacteria in the bottom 30 cm of the sea ice of 1.1 $\times$ 10^5 cells ml^{-1} sea ice corresponding to 1.2 $\times$ 10^6 cells ml^{-1} brine. The 95% confidence interval was, in all series, 0.18 $\times$ 10^5 cells ml^{-1} sea ice (lower limit) and 4.1 $\times$ 10^5 cells ml^{-1} sea ice (upper limit). Identical numbers were obtained when checking for nitrate-respiring bacteria. In all dilution series, gas production was observed. Moreover, $^{15}NO_3^-$-incubated samples showed ^{15}N-N_2 production after 24 h and confirmed the presence of denitrifying bacteria.

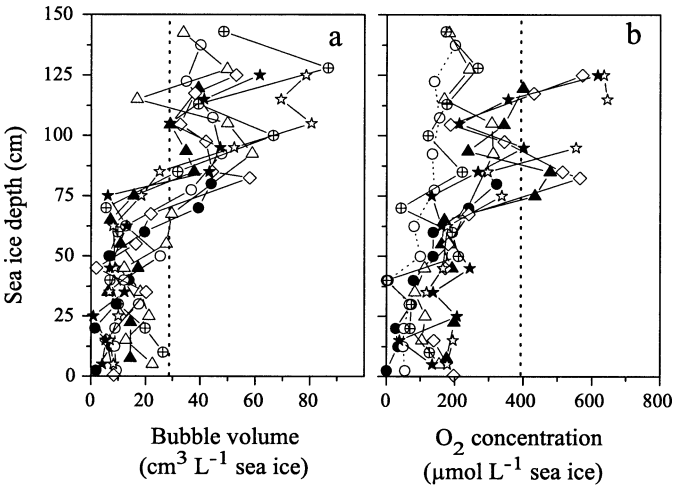

Fig. 5. Oxygen in Young Sound sea ice. (a) Bubble (gas) volume and (b) total O_2 concentration in sea ice. Vertical dotted line in panel a represents expected gas volume at −2°C and a bulk salinity of 4. Vertical dotted line in panel b represents atmospheric O_2 saturation at −1.8°C and salinity of 33. Symbols as in Fig. 2.

Discussion

Sea ice conditions in Young Sound during 28 May–12 June were characterized by surface ablation of the snow pack with meltwater production rates of 6 mm d^{-1} (Fig. 1). This corresponds to observations made on first-year ice in the northern Chukchi Sea, where a meltwater production of 1–10 mm d^{-1} was observed during the initial Stage I phase of sea-ice melting (Eicken et al. 2002). Due to the solid freshwater ice layer present immediately below the snow layer in Young Sound, meltwater percolating down through the snow made the lower parts of the snow pack wet (Fig. 1). The temperature increase within the sea ice during the investigation period lowered bulk salinities and increased the brine volume (Fig. 2). An increase in brine volume will increase sea-ice permeability (Freitag 1999), and especially on the last sampling dates, the brine volume greatly increased in the lower 25 cm of the sea ice, indicating the onset of bottom sea-ice ablation (Fig. 2).

Oxygen conditions in sea ice—The observation that the total O_2 concentration was zero in some areas of the ice and that most of the lower 75 cm of the sea-ice matrix had O_2 concentrations much lower than expected from atmospheric saturation at −1.8°C and a salinity of 33 at which sea ice forms, suggests that O_2 is lost from the sea ice (Fig. 5). Recently, it has been shown that brine leaking out of growing sea ice is supersaturated whereas melting water is undersaturated with respect to O_2 (Glud et al. 2002). Thus, O_2 and other gases (N_2, Ar, CO_2) essentially behave in the same way as ionic solutes that are liberated to the brine during freezing (Eide and Martin 1975; Wakatsuchi and Ono 1983). Therefore, part of the O_2 in the matrix of the sea ice had been lost to the underlying water during ice growth prior to the investigation period.

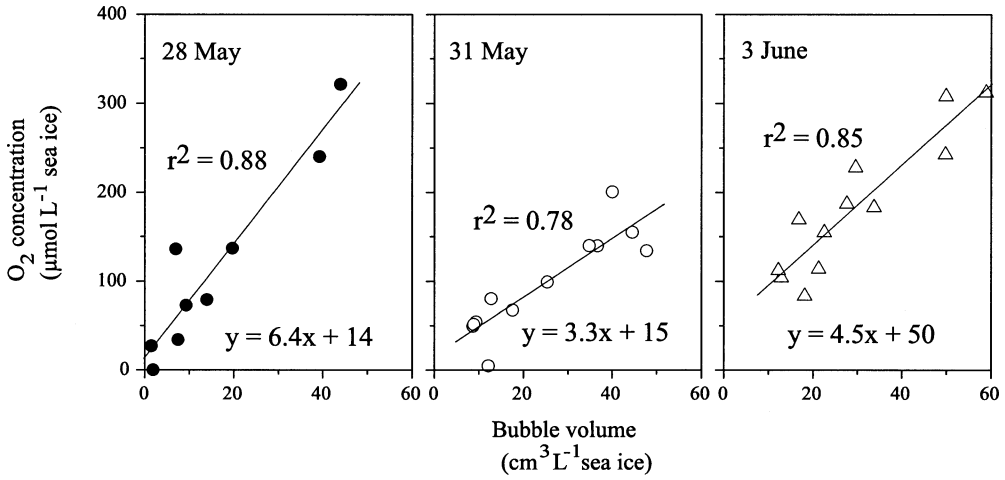

Fig. 6. Oxygen concentration as a function of bubble volume during the first three sampling dates. Symbols as in Fig. 2.

The fact that O_2 concentrations in the sea ice were initially highly correlated with the gas volume of the sea ice and followed the same vertical distribution (Fig. 6) suggests that a major part of the O_2 in the sea-ice matrix was trapped within gas bubbles that develop during the freezing process. Recent laboratory studies with O_2 microsensors (Glud et al. 2002) and O_2 micro-optodes (Mock et al. 2002) support this suggestion. Assuming that gas formation occurs from O_2, N_2, Ar, and CO_2 freezing out simultaneously and that their proportions are determined by their solubility in the brine, it follows that the expected fraction of O_2 within the gas is ~1/3. This is a reasonable assumption because (1) the solubilities of O_2, N_2, and Ar behave in a similar manner with varying temperature and salinity (Weiss 1970), (2) the amount of free CO_2 is bound to be low given the temperature, pH, and salinity regimes that can occur in the lower 0.75 m of the sea ice in Young Sound and (3) the solubility of CO_2 is high in seawater compared with O_2, N_2, and Ar (Weiss 1974; Lueker et al. 2000). The expected O_2 concentration within the gas can then be estimated using the measured bubble volumes and the fraction of O_2 within the bubbles. It turns out that the measured O_2 concentrations are ~30% of the theoretically calculated concentrations, implying that gas bubbles within the sea ice are highly undersaturated with respect to O_2.

Given the nature of the complex brine pockets and channel structure in sea ice (Weissenberger et al. 1992), the gas bubbles in the sea-ice matrix are a mixture of isolated bubbles surrounded by solid ice and of bubbles in contact with the brine channels. If the bubbles are in equilibrium with the brine, they will represent an O_2 source for O_2-consuming bacteria within the brine system. However, with a net O_2 consumption in the sea ice of 13 μmol L^{-1} sea ice day^{-1}

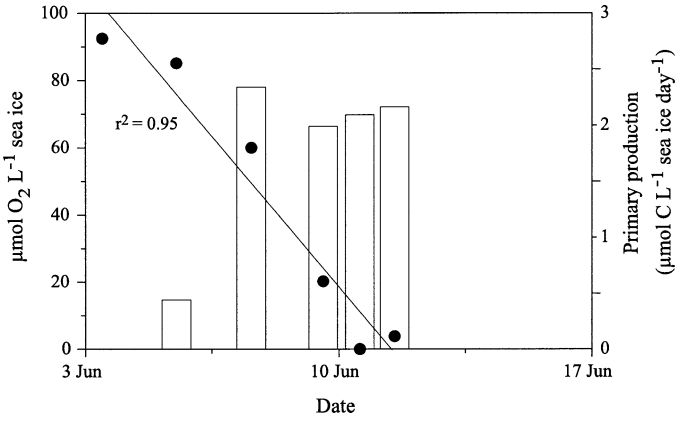

Fig. 7. Primary production (bars) and O_2 concentration in the bottom 30 cm of the sea ice on different dates in Young Sound (circles) in the gas-tight bag incubations. Line represents linear regression of O_2 concentration in bags ($r^2 = 0.95$, $P = 0.013$).

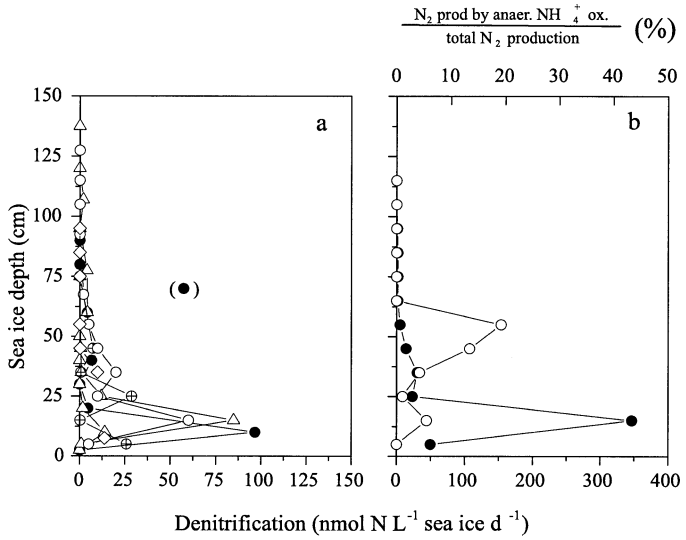

Fig. 8. Anaerobic N_2 production in (a) Young Sound first-year ice and (b) Greenland Sea ice floe. Only denitrification was observed at the Young Sound location. Symbols for panel a are as in Fig. 2. In panel b, closed symbols represent denitrification while open symbols represent N_2 production by anaerobic NH_4^+ oxidation as a percentage of total N_2 production. Note the scale difference between panels a and b.

(Fig. 7), the ice incubated gas-tight bag became anoxic within 1 week, showing that gas bubbles could not sustain aerobic respiration within the brine system over a period of any length. In our in situ gas-tight bag incubations, all O_2 contained within the isolated bubbles became available to bacterial consumption due to slightly higher melting of sea ice in the bags as compared with the surrounding sea ice during the late phase of incubation (Fig. 7).

As sea ice is in contact with the atmosphere and underlying seawater, transport of O_2 into the sea-ice matrix may occur from both of these phases. Given the brine volume of 0.1–0.2 from 28 May–10 June (Fig. 2), an O_2 concentration in the water column of 382 μmol L^{-1} and the net O_2 consumption rate within the brine of 73–130 μmol L^{-1} brine day^{-1}, O_2 can be calculated to penetrate only ~0.5 cm into the sea ice if molecular diffusion were the sole transport mechanism (Sten-Knudsen 2002). Both freezing and melt conditions, however, will affect the transport of brine (Eicken et al. 2002). Freezing conditions only occurred throughout the sea-ice matrix on the initial sampling date in Young Sound followed by melt conditions during the remaining investigation period (Fig. 2a). At present, we have no direct measurements of the volume transport of brine or meltwater, but in sea ice as thick as the Young Sound and Greenland Sea ice, sea-ice growth is very slow, and consequently brine volume flux due to sea-ice growth is very small (Wakatsuchi and Ono 1983). Active melting of sea ice, however, will affect the transport in the brine channels. Given the temperature increase of 1°C ($P < 0.001$, $r^2 = 0.88$) and concurrent decrease in bulk salinity of 1 ($P < 0.001$, $r^2 = 0.80$) corresponding to a decrease in brine salinity from 42 to 19 ($P < 0.001$, $r^2 = 0.86$) in the lower 0.5 m of the sea ice from 28 May–12 June (Fig. 3), a transport of 9.0×10^{-6} cm s^{-1} meltwater is required to account for the salinity dilution. As melted sea ice, including bubbles, contains ~120 μmol O_2 L^{-1} (Figs. 5b, 7), a transport of 9.0×10^{-6} cm s^{-1} implies that, on average, O_2 would only move 3.6 cm from the melting point in the brine system before being consumed, assuming homogeneous O_2 consumption in the bottom sea ice. Performing the same calculation based on data from 28 May–6 June (brine salinity decrease from 42 to 35; $P < 0.001$, $r^2 = 0.95$) where active bacterial denitrification took place (Figs. 3, 8) yields a lower meltwater transport of 3.2×10^{-6} cm s^{-1}, implying that O_2 in melted water is consumed before moving 2.2 cm. Thus, even though brine transport (and O_2 transport) may be highly heterogeneous in the sea ice due to the complex brine pockets and channel structure, brine volume flow due to meltwater percolation found in the present study period cannot prevent the development of anoxia inside the sea-ice brine system.

Anaerobic N_2 production in sea ice—Anoxic conditions combined with high concentrations of NO_3^- and organic carbon (Fig. 4) concentrations within the brine system make brine channels and pockets a potential site for nitrate reduction. Bacterial denitrification activity was observed in both investigated sea-ice types with highest activities in the lower 25 cm (Fig. 8). A decreasing trend in denitrification activity seemed to occur from 28 May to 10 June due to the onset of ice melt, and activity ceased during the final two sampling dates, presumably due to washout of organisms caused by the high ablation of bottom sea ice and high brine volumes increasing permeability of the bottom layer on these sampling dates. It is likely that denitrification activity also occurred before 28 May as active biological activity in sea ice has been observed to occur down to −11°C (Krembs et al. 2002). However, more work is needed in order to elucidate the seasonal variation in the anaerobic denitrification activity of sea ice.

To our knowledge, only one study of denitrification capacity in sea ice has been published earlier (Kaartokallio 2001). The distribution of activity in the present study is in agreement with recent findings from the Baltic Sea, where the highest activity of N_2O production was obtained in anaerobic cultures isolated from the bottom 10–30 cm of the ice (Kaartokallio 2001). The elevation in denitrification activity in the latter study was associated with accumulation of NO_2^- in sea ice.

Integrating the measured denitrification activities in Fig. 8 yields a rate of 10–45 μmol N m^{-2} sea ice d^{-1}, which corresponds to 7–50% of sediment activity measured at different depths in the area during 1996 and 2002 (Rysgaard et al. 1998; Glud et al. 2000; Rysgaard et al. unpubl. data). Compared with the integrated NO_3^- pool in the sea ice of ~1,400 μmol m^{-2} (Fig. 4c), the denitrification activity will deplete the pool in 30–140 d if it is not replaced. Because denitrification rates in the present study are based on melted ice core measurements under anoxic conditions, they do not represent an intact and undisturbed sea-ice matrix where both oxic and anoxic conditions prevail in a complex structure. Thus, our estimates do not include the coupling between nitrification and denitrification. At present, we have no measurements of nitrification in sea ice from our study areas. However, nitrification has been reported to occur in Antarctic sea ice (Priscu et al. 1990) and one would expect the process to occur in the vicinity of O_2-containing bubbles, close to the sea-ice–water interface, and in areas where large brine channels are in contact with O_2-containing water.

Although no significant N_2 production by anaerobic NH_4^+ oxidation (anammox) could be measured in Young Sound, the process accounted for up to 19% of the total N_2 production in the deeper layers of the sea-ice floe in the Greenland Sea (Fig. 8). The higher proportion of anammox to N_2 production in the multiyear sea ice could be due to the more stable environment of multiyear sea ice as compared with annual sea ice. This may favor the apparently slow-growing anammox bacteria that in general seem to prefer more stable environments (Jetten et al. 2001). However, more studies are needed to evaluate this hypothesis. The anammox process was first discovered in a wastewater treatment plant (Mulder et al. 1995), but recent studies have shown that anammox may be a significant process in marine sediments also, where it may account for more than 60% of anaerobic N_2 production (Thamdrup and Dalsgaard 2002). Although the proportion of anammox to total N_2 production in some ice floe layers was significant, the integrated rate only accounted for 0–2.3 μmol N m^{-2} d^{-1}, corresponding to 0–5% of total NO_3^- reduction at the investigated localities.

We found relatively high numbers of anaerobic nitrate-reducing bacteria (1.1×10^5 ml^{-1} sea ice corresponding to

1.2×10^6 ml^{-1} brine) in the bottom 30 cm of the sea ice in Young Sound, supporting the denitrification measurements above (Fig. 8). We are not aware of other published values of anaerobic nitrate-reducing bacterial numbers from sea ice but, although not quantified, bacterial strains of denitrifying species have been isolated from Antarctic sea ice (Gosink and Staley 1995; Bowman et al. 1997). However, bacterial numbers from the Young Sound ice compare with numbers reported from sediments where active denitrification activity takes place (Dultseva and Odintsov 1991; Scholten et al. 2002). Furthermore, they compare with reported values of total bacterial numbers from Arctic sea ice ($0.4–36.7 \times 10^5$ cells ml^{-1} sea ice; Gradinger and Zhang 1997 and references therein) and our findings suggest that anaerobic nitrate-reducing bacteria may account for a substantial fraction of the total bacterial assemblage in sea ice.

Analyses of the recent history of sea-ice extent from satellite data show that sea ice in the Arctic has declined at a decadal rate of 2.8–3% since 1978 (Bjørgo et al. 1997), with a more rapid recent decline of 4.3% taking place between 1987 and 1994 (Johannessen et al. 1995). Although sea-ice extent since 1978 shows an apparently fairly stable annual cycle of large amplitude, a downward trend occurs for every season of the year and a mean annual loss of ice area in the Arctic has been estimated at $34{,}300 \pm 3{,}700$ km^2 (Parkinson et al. 1999). This considerable decrease in ice cover affects the biological productivity and mineralization processes of arctic areas. In the present study, we have provided evidence for anoxic conditions and active denitrification within sea ice. Consequently, it may be speculated that, along with increasing light availability, decreasing ice cover would lead to less nitrogen removal from Arctic areas, allowing further stimulation of pelagic primary production.

We have established that aerobic and anaerobic activity may occur simultaneously within intact ice cores characterized by heterogeneously distributed active microzones. However, sea ice is an extremely complex medium with which to work. It is practically impossible to measure microbial abundance or activity without disturbing the intact ice structure. Further investigations resolving the microzonation are required, but the findings of O_2 depletion and active denitrification in sea ice change our present understanding of carbon and nutrient cycling in polar regions.

References

BJØRGO, E., O. M. JOHANNESSEN, AND M. W. MILES. 1997. Analysis of merged SMMR-SSMI time series of Arctic and Antarctic sea ice parameters 1978–1995. Geophys. Res. Lett. **24:** 413–416.

BOWMAN, J. P., S. A. MCCAMMON, M. V. BROWN, D. S. NICHOLS, AND T. A. MCMEEKIN. 1997. Diversity and association of psychrophilic bacteria in Antarctic sea ice. Appl. Environ. Microbiol. **63:** 3068–3078.

COX, G. F. N., AND W. F. WEEKS. 1983. Equations for determining the gas and brine volumes in sea-ice samples. J. Glaciol. **29:** 306–316.

DALSGAARD, T., AND B. THAMDRUP. 2002. Factors controlling anaerobic ammonium oxidation with nitrite in marine sediments. Appl. Environ. Microbiol. **68:** 3802–3808.

DEVOL, A. H., L. A. CODISPOTI, AND J. P. CHRISTENSEN. 1997. Summer and winter denitrification rates in western Arctic shelf sediments. Cont. Shelf Res. **17:** 1029–1050.

DULTSEVA, O. A., AND V. S. ODINTSOV. 1991. Number and activity of denitrifying bacteria in soft sediments of Vostok Bay, Sea of Japan. Biologiya Morya-Marine Biol. **5:** 56–62.

EICKEN, H., H. R. KROUSE, D. KADKO, AND D. K. PEROVICH. 2002. Tracer studies of pathways and rates of meltwater transport through Arctic summer sea ice. J. Geophys. Res. **107**(C10) art. no. 8046, Sep–Oct.

EIDE, L. I., AND S. MARTIN. 1975. The formation of brine drainage features in young sea ice. J. Glaciol. **14:** 137–154.

FREITAG, J. 1999. The hydraulic properties of Arctic sea ice—implications for the small-scale particle transport (in German). Ber. Polarforsch. **325,** 150 pp.

GLOERSEN, P., W. J. CAMPBELL, D. J. CAVALIERI, J. C. COMISO, C. L. PARKINSON, AND H. J. ZWALLY. 1992. Arctic and Antarctic sea ice, 1978–1987: Satellite passive-microwave observations and analysis. National Aeronautics and Space Administration, Rep. NASA SP-511.

GLUD, R. N., N. RISGAARD-PETERSEN, B. THAMDRUP, AND S. RYSGAARD. 2000. Carbon mineralization in a high-Arctic fjord, Northeast Greenland. Mar. Ecol. Prog. Ser. **206:** 59–71.

———, S. RYSGAARD AND M. KÜHL. 2002. A laboratory study on O_2 dynamics and photosynthesis in ice algal communities: Quantification by microsensors, O_2 exchange rates, ^{14}C incubations and PAM fluorometer. Aquat. Microb. Ecol. **27:** 301–311.

GOSINK, J. J., AND J. T. STALEY. 1995. Biodiversity of gas vacuolate bacteria from Antarctic sea ice and water. Appl. Environ. Microbiol. **61:** 3486–3489.

GRADINGER, R., AND Q. ZHANG. 1997. Vertical distribution of bacteria in Arctic sea ice from the Barents and Laptev Seas. Polar Biol. **17:** 448–454.

GRASSHOFF, K., M. ERHARDT, AND K. KREMLING. 1983. Methods of seawater analysis. 2nd revised and extended version. Weinheim and Verlage Chemie.

HANSEN, J. W., B. THAMDRUP, AND B. B. JØRGENSEN. 2000. Anoxic incubation of sediment in gas-tight plastic bags: A method for biogeochemical process studies. Mar. Ecol. Prog. Ser. **208:** 273–282.

HØJBERG, O., N. P. REVSBECH, AND J. M. TIEDJE. 1994. Denitrification in soil aggregates analyzed with microsensors for nitrous oxide and oxygen. Soil Sci. Soc. Am. J. **58:** 1691–1698.

JETTEN, S. M., M. WAGNER, J. FUERST, M. VAN LOOSDRECHT, G. HUENEN, AND M. STROUS. 2001. Microbiology and application of anaerobic ammonium oxidation ('anammox') process. Environ. Biotech. **12:** 293–288.

JOHANNESSEN, O. M., M. MILES, AND E. BJØRGO. 1995. The Arctic's shrinking sea ice. Nature **376:** 126–127.

KAARTOKALLIO, H. 2001. Evidence for active microbial nitrogen transformations in sea ice (Gulf of Bothnia, Baltic Sea) in midwinter. Polar Biol. **24:** 21–28.

KREMBS, C., H. EICKEN, K. JUNGE, AND J. W. DEMING. 2002. High concentrations of exopolymeric substances in Arctic winter sea ice: Implications for the polar ocean carbon cycle and cryoprotection of diatoms. Deep-Sea Res. **49:** 2163–2181.

LEPPÄRANTA, M., AND T. MANNINEN. 1988. The brine and gas content of sea ice with attention to low salinities and high temperatures. Finnish Inst. Marine Res. Internal Rep. 88-2.

LUEKER, T. J., A. G. DICKSON, AND C. D. KEELING. 2000. Ocean PCO_2 calculated from dissolved inorganic carbon, alkalinity and equations for K_1 and K_2: Validation based on laboratory measurements of CO_2 in gas and seawater at equilibrium. Mar. Chem. **70:** 105–119.

MOCK, T., AND OTHERS. 2002. Micro-optodes in sea ice: A new

approach to investigate oxygen dynamics during sea ice formation. Aquat. Microb. Ecol. **29:** 297–306.

MULDER, A., A. A. VAN DE GRAAF, L. A. ROBINSON, AND J. G. KUENEN. 1995. Anaerobic ammonium oxidation in a denitrifying fluidized reactor. FEMS Microbiol. Ecol. **16:** 177–184.

NIELSEN, L. P. 1992. Denitrification in sediment determined from nitrogen isotope pairing. FEMS Microbiol. Ecol. **86:** 357–362.

PARKINSON, C. L., D. J. CAVALIERI, P. GLOERSEN, H. J. ZWALLY, AND J. C. COMISO. 1999. Arctic sea ice extents, areas and trends, 1978–1996. J. Geophys. Res. **104:** 20837–20856.

PETRI, R., AND J. F. IMHOFF. 2001. Genetic analysis of sea-ice bacterial communities of the Western Baltic Sea using an improved double gradient method. Polar Biol. **24:** 252–257.

PRISCU, J. C., M. T. DOWNES, L. R. PRISCU, A. C. PALMISANO, AND C. W. SULLIVAN. 1990. Dynamics of ammonium oxidizer activity and nitrous oxide (N_2O) within and beneath antarctic sea ice. Mar. Ecol. Prog. Ser. **62**: 37–46

RISGAARD-PETERSEN, N., AND S. RYSGAARD. 1995. Nitrate reduction in sediments and waterlogged soil measured by ^{15}N techniques, p. 287–310. *In* K. Alef and P. Nannipieri [eds.], Methods in applied soil microbiology and biochemistry. Academic.

RYSGAARD, S., B. THAMDRUP, N. RISGAARD-PETERSEN, P. BERG, H. FOSSING, P. B. CHRISTENSEN, AND T. DALSGAARD. 1998. Seasonal carbon and nitrogen mineralization in the sediment of Young Sound, Northeast Greenland. Mar. Ecol. Prog. Ser. **175:** 261–276.

———, M. KÜHL, R. N. GLUD, AND J. W. HANSEN. 2001. Biomass, production and horizontal patchniness of sea ice algae in a high-arctic fjord (Young Sound, NE Greenland). Mar. Ecol. Prog. Ser. **223:** 15–26.

SCHOLTEN, J. C. M., P. M. VAN BODEGOM, J. VOGELAAR, A. VAN ITTERSUM, K. HORDIJK, W. ROELODSEN, AND A. J. M. STAMS. 2002. Effect of sulfate and nitrate on acetate conversion by anaerobic microorganisms in a freshwater sediment. FEMS Microbiol. Ecol. **42:** 375–385.

STALEY, J. T., AND J. J. GOSINK. 1999. Poles apart: Biodiversity and biogeography of sea ice bacteria. Annu. Rev. Microbiol. **53:** 189–215.

STEN-KNUDSEN, O. 2002. Biological membranes: Theory of transport, potentials and electrical impulses. Cambridge Univ. Press.

THAMDRUP, B., AND T. DALSGAARD. 2002. Production of N_2 through anaerobic ammonium oxidation coupled to nitrate reduction in marine sediments. Appl. Environ. Microbiol. **68:** 1312–1318.

TIEDJE, J. M. 1988. Ecology of denitrification and dissimilatory nitrogen reduction to ammonium, p. 179–244. *In* A. J. B. Zehnder [ed.], Biology of anaerobic microorganisms. Wiley.

THOMAS, D. N., R. J. LARA, H. EICKEN, G. KATTNER, AND A. SKOOG. 1995. Dissolved organic matter in arctic multi-year sea ice during winter: Major components and relationship to ice characteristics. Polar Biol. **15:** 477–483.

WAKATSUCHI, M., AND N. ONO. 1983. Measurements of salinity and volume of brine excluded from growing sea ice. J. Geophys. Res. **88:** 2943–2951.

WEISS, R. F. 1970. The solubility of nitrogen, oxygen and argon in water and seawater. Deep-Sea Res. **17:** 721–735.

———. 1974. Carbon dioxide in water and seawater: The solubility of a non-ideal gas. Mar. Chem. **2:** 203–215.

WEISSENBERGER, J., G. DIECKMANN, R. GRADINGER, AND M. SPINDLER. 1992. Sea ice: A cast technique to examine and analyze brine pockets and channel structure. Limnol. Oceanogr. **37:** 179–183.

WIDDEL, F., AND F. BAK. 1992. Gram-negative mesophilic sulfate-reducing bacteria, p. 3352–3378. *In* A. Balows, H. G. Trüper, M. Dworkin, W. Harder, and K.-H. Schleifer [eds.], The prokaryotes, V. 4. Springer.

Received: 14 March 2003
Accepted: 23 July 2003
Amended: 5 August 2003